Ab initio study of the split silicon-vacancy defect in diamond: Electronic structure and related properties

Adam Gali[1,2,*] and Jeronimo R. Maze[3,†]

[1]*Wigner Research Centre for Physics, Hungarian Academy of Sciences, P.O. Box 49, H-1525, Budapest, Hungary*

[2]*Department of Atomic Physics, Budapest University of Technology and Economics, Budafoki út 8, H-1111 Budapest, Hungary*

[3]*Faculty of Physics, Pontificia Universidad Católica de Chile, Santiago 7820436, Chile*

(Received 13 October 2013; published 16 December 2013)

The split silicon-vacancy (SiV) defect in diamond is an electrically and optically active color center. Recently, it has been shown that this color center is bright and can be detected at the single defect level. In addition, the SiV defect shows a nonzero electronic spin ground state that potentially makes this defect an alternative candidate for quantum optics and metrology applications beside the well-known nitrogen-vacancy color center in diamond. However, the electronic structure of the defect, the nature of optical excitations and other related properties are not well understood. Here we present advanced *ab initio* study on SiV defect in diamond. We determine the formation energies, charge transition levels, and the nature of excitations of the defect. Our study unravels the origin of the dark or shelving state for the negatively charged SiV defect associated with the 1.68-eV photoluminescence center.

DOI: 10.1103/PhysRevB.88.235205 PACS number(s): 61.72.J−, 61.82.Fk, 71.15.Mb, 76.30.−v

I. INTRODUCTION

The 1.68-eV photoluminescence (PL) center in diamond was reported many decades ago[1] and later it was assumed[2] that silicon impurities were involved in this center. This was confirmed by PL measurements at cryogenic temperature on Si-doped chemical vapor deposition (CVD) polycrystalline diamond samples where the fine structure of the 1.68-eV PL center could be detected.[3] A 12-line fine structure is observed close to 1.68 eV, and this can be divided into three similar groups, each containing four components. The relative strengths of the optical absorption for the three groups of lines are found to be the same as the ratio of the abundances of the natural isotopes of silicon, ^{28}Si, ^{29}Si, and ^{30}Si[3]. The 4-line fine structure for an individual Si isotope is assigned to doublet levels both in the ground and excited states which split by about 48 and 242 GHz, respectively.[3] It has been assumed that this small splitting might be explained by dynamic Jahn-Teller effect[3] and/or by spin-orbit effect.[4]

Recently, single photon emission from 1.68-eV PL center has been demonstrated.[5–8] Its zero-phonon line (ZPL) with 5 nm width even at room temperature and the near-infrared emission makes this PL center a very attractive candidate for quantum optics[5–7] and biomarker[9] applications.

Spin-polarized local density approximation (LDA) within density functional theory (DFT) calculations with a very small cluster containing ∼70 carbon atoms concluded (see Ref. 4 and references for LDA functional therein) that the negatively charged split-vacancy form (see Fig. 1) of the silicon-vacancy (SiV) defect (SiV^-) is responsible for the 1.68-eV PL center. They exclude the neutral SiV defect (SiV^0) as a good candidate because its ground state is an orbital singlet that would not show the dynamic Jahn-Teller effect.[4] This model was later disputed based on a semiempirical restricted open-shell Hartree-Fock cyclic cluster model calculation where they claimed that tunneling of the Si atom along the symmetry axis may occur for a SiV^0 defect that can explain the doublet line in the ground state without invoking a dynamic Jahn-Teller effect.[10]

The fingerprint of SiV^0 was found by electron paramagnetic resonance (EPR) studies.[11–13] The KUL1 center with $S = 1$ high-spin ground state and D_{3d} symmetry[13] was recently associated with a SiV^0 defect where 216-atom LDA supercell calculations produce relatively good agreement with the measured ^{13}C and ^{29}Si hyperfine couplings (see Table I). Very recently, thorough EPR and PL studies have been carried out to correlate the KUL1 EPR center with an 1.31-eV PL center and its relation to the 1.68-eV PL center.[14] The final conclusion was that SiV^0 has a ZPL at 1.31 eV, whereas SiV^- has a ZPL at 1.68 eV. Photoconductivity measurements[15] and photoionization measurements[14] indicate that the adiabatic (thermal) charge transition level of the $(-|0)$ level of the SiV defect is at $\sim E_{\mathrm{VBM}} + 1.5$ eV, where VBM is the valence band (VB) edge.

While the interpretation of the recent measurements[14] is very plausible, still no *ab initio* theory was able to conclusively support the assignment of 1.68-eV center with the negatively charged SiV defect. LDA or any semilocal generalized gradient approximation (GGA) functionals suffer from the band-gap error[16,17] which inhibits to directly compare the calculated and experimental ZPL energies. Recent advances in DFT functionals have made it possible to accurately calculate ZPL energies and charge transition level of defects in diamond and other semiconductors.[18–20] In this paper, we apply this theory to study the charge transition levels and the ZPL energies of SiV defect in diamond. These calculations yield the position and nature of defect states in host diamond and are able to reveal the nature of the shelving state in a 1.68-eV PL center.

Our paper is organized as follows. In Sec. II we describe briefly the *ab initio* method that we applied to study the electronic structure and excitations of the SiV defect. In Sec. III we describe the structure and the basic defect level scheme of SiV defect by group theory. Here we combine the results from *ab initio* calculations with group-theory considerations in order to identify the order of important defect states and the charge state relevant for the most important 1.68-eV PL center. We discuss the results then we conclude and summarize the results in Sec. IV.

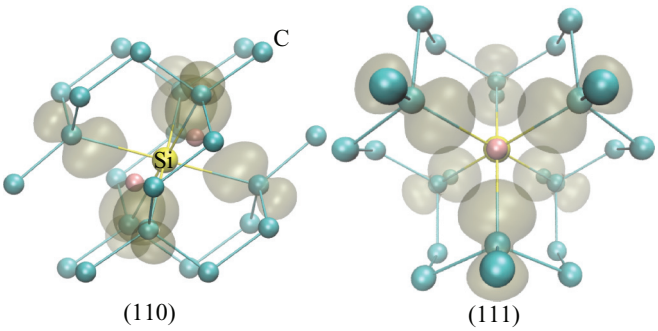

FIG. 1. (Color online) The split-vacancy structure of the SiV defect and the calculated spin density in neutral charge state. The isosurface of spin density is 0.05. The defect has D_{3d} symmetry with the symmetry axis of [111] direction. The lattice sites of the missing carbon atoms are depicted by the smallest (pink) balls.

II. METHOD

The present calculations have been carried out in the framework of the generalized Kohn-Sham theory,[21] by using the screened hybrid functional HSE06 of Heyd, Ernzerhof, and Scuseria with the original parameters (0.2 Å^{-1} for screening and 25% mixing).[22,23] HSE06 in diamond happens to be nearly free of the electron self-interaction error and is capable of providing defect levels and defect-related electronic transitions within ~0.1 eV to experiment.[18–20]

We have used the Vienna Ab Initio Simulation Package VASP 5.3.2 with the projector augmented wave[24] (PAW) method (applying projectors originally supplied to the 5.2 version).[25] To avoid size effects as much as possible, a 512-atom supercell was used in the Γ approximation for defect studies. Parameters for the supercell calculations were established first by using the GGA exchange of Perdew, Burke, and Ernzerhof (PBE)[26] in bulk calculations on the primitive cell with an 8 × 8 × 8 Monkhorst-Pack (MP) set for Brillouin-zone sampling.[27] (Increasing the MP set to 12 × 12 × 12 has changed the total energy by <0.002 eV.) Constant volume relaxations using a cutoff of 370(740) eV in the plane-wave expansion for the wave function (charge density) resulted in an equilibrium lattice parameter of $a_{\mathrm{PBE}} = 3.570$ Å. Increasing the cutoff to 420(840) eV has changed the lattice constant by only 0.003 Å. Therefore, considering the demands of the supercell calculations, the lower cutoff was selected. The HSE06 calculation with the 8 × 8 × 8 MP set and 370(740)-eV cutoff resulted in the lattice constant $a_{\mathrm{HSE}} = 3.545$ Å, indirect band gap of $E_g = 5.34$ eV, in good agreement with the experimental values of $a = 3.567$ Å and $E_g = 5.48$ eV (see, e.g., Ref. 28). Due to the different choice of the basis, the HSE06 values presented here differ somewhat from those in Refs. 18, 19, and 28, but tests on the negatively charged nitrogen-vacancy (NV) center have shown that the higher cutoff would cause only negligible difference in the equilibrium geometry of that defect too. Defects in the supercell were allowed to relax in constant volume until the forces were below 0.01 eV/Å.

TABLE I. Calculated and measured hyperfine constants (A) for KUL1 EPR center and neutral SiV defect in diamond. The KUL1 EPR center data was taken from Ref. 13. Previous theoretical results are taken from Ref. 34, carried out by LDA 216-atom supercell calculation without taking into account the core polarization (LDA-nocp). The present theoretical values are obtained by HSE06 functional in 512-atom supercell where the contribution of the spin polarization of core electrons to the Fermi-contact term in ^{13}C is 26% of the total (HSE06-cp). Θ is the angle between the symmetry axis ([111] direction) and the parallel component of the hyperfine constant $A_{||}$.

Interaction	$A_{\|\|}$ (MHz)	$A_{\perp}$ (MHz)	Θ (°)
^{13}C (experiment)[a]	66.2	30.2	35.3
^{13}C (LDA-nocp)[b]	51	12	33.3
^{13}C (HSE06-cp)	68	28	34.6
^{29}Si (experiment)[a]	76.3	78.9	0
^{29}Si (LDA-nocp)[b]	78	82	0
^{29}Si (HSE06-cp)	92	97	0

[a]Reference 13.
[b]Reference 34.

We calculated the hyperfine tensors of ^{13}C and ^{29}Si isotopes within PAW formalism[29] as implemented in VASP 5.3.3 package. Here, we applied a larger 500(1000)-eV cutoff for the plane-wave (charge density) expansion. The hyperfine tensor ($A_{ij}^{(J)}$) between the electron spin density $\sigma(\mathbf{r})$ of an electron spin S, and the nonzero nuclear spin I of nucleus J may be written as

$$A_{ij}^{(J)} = \frac{1}{2S}\mu_e\mu_J\left[\frac{8\pi}{3}\int \delta(\mathbf{r}-\mathbf{R}_J)\sigma(\mathbf{r})d\mathbf{r} + W_{ij}(\mathbf{R}_J)\right], \quad (1)$$

where the first term within the square brackets is the so-called (isotropic) Fermi-contact term, and

$$W_{ij}(\mathbf{R}) = \int\left[\frac{3(\mathbf{r}-\mathbf{R})_i(\mathbf{r}-\mathbf{R})_j}{|\mathbf{r}-\mathbf{R}|^5} - \frac{\delta_{ij}}{|\mathbf{r}-\mathbf{R}|^3}\right]\sigma(\mathbf{r})d\mathbf{r} \quad (2)$$

represents the (anisotropic) magnetic dipole-dipole contribution to the hyperfine tensor. μ_J is the nuclear Bohr magneton of nucleus J and μ_e the electron Bohr magneton. The Fermi-contact term is proportional to the magnitude of the electron spin density at the center of the nucleus which is equal to one-third of the trace of the hyperfine tensor, $\frac{1}{3}\sum_i A_{ii}$. The Fermi-contact term arises from the spin density of unpaired electrons with s character and can be quite sizable. The spin density built up from unpaired electrons of p character yields the dipole-dipole hyperfine coupling. The fraction of Fermi-contact and dipole-dipole terms implicitly provides information about the character of the wave function of the unpaired electron as well as the corresponding nuclei (via γ_J). According to our recent study,[30] the contribution of the spin polarization of core electrons to the Fermi-contact hyperfine interaction[31] is significant for ^{13}C isotopes; thus, we include this term in the calculation of hyperfine tensors.

The excitation energies were calculated within constrained DFT method that was successfully applied to the NV center in diamond.[18] In this method one can calculate the relaxation energy of the nuclei due to optical excitation.

The formation energy of the defect with defect charge state q is defined as

$$E_{\mathrm{form}}^q = E_{\mathrm{tot}}^q - n_{\mathrm{C}}\mu_{\mathrm{C}} - \mu_{\mathrm{Si}} + qE_{\mathrm{F}} + \Delta V(q) \quad (3)$$

by ignoring the entropy contributions, where $E^q_{\rm tot}$ is the total energy of the defect in the supercell, $E_{\rm VBM}$ is the calculated energy of VBM in the perfect supercell, $\mu_{\rm C}$ and $\mu_{\rm Si}$ are the chemical potentials of C and Si atoms in diamond, respectively, with $n_{\rm C}$ number of C atoms in the supercell, $E_{\rm F}$ is the chemical potential of the electron, i.e., the Fermi-level, and $\Delta V(q)$ is the correction needed for charged supercells. The thermal charge transition level between the defect charge states of q and $q+1$ is the position of the Fermi level ($E_{\rm F}$) in the fundamental band gap of diamond, where the formation energies are equal in these charge states. This condition simplifies to a difference in the total energies in their respective charge states as

$$E_{\rm F} = E^q_{\rm tot} - E^{q+1}_{\rm tot} + \Delta V(q) - \Delta V(q+1), \qquad (4)$$

where $E_{\rm F}$ is referenced to the calculated $E_{\rm VBM}$. For comparison of different defect configurations and charge states, the electrostatic potential alignment and the charge correction scheme of Lany and Zunger was applied for $\Delta V(q)$.[32] Recently, this scheme was found to work best for defects with medium localization.[33]

III. RESULTS

We first study the structure and the obtained defect levels by HSE06 calculation. Then, we apply group theory in order to explain the symmetry of the defect states. We use the calculated thermal ionization energies, excitation energies, and hyperfine couplings to identify the 1.31- and 1.68-eV PL centers. We also discuss the results, comparing them to the experiments.

A. *Ab initio* results and group-theory analyses of the defect states for neutral SiV defect in diamond

We first calculated the neutral defect SiV^0 by substituting the C atom with a Si atom adjacent to a nearby vacancy. The Si automatically left the substitutional site creating a split-vacancy configuration which may be described as a Si atom placed in a divacancy where the position of the Si atom is equidistant from the two vacant sites (see Fig. 1). The position of a Si atom is a bond center position which is an inversion center of perfect diamond lattice. In our special coordinate frame the two vacant sites reside along the [111] direction of the lattice which has a C_3 rotation axis. The symmetry of the defect may be described as $C_{3v} \times i$ or D_{3d}, where i is the inversion. We note that the NV center has C_{3v} symmetry with no inversion. The defect has $S = 1$ high-spin ground state. This finding agrees with the LDA calculations.[4,34] After establishing the symmetry of the defect one can apply group-theory analysis for this defect.[4,14,34] One can build the defect states of this defect as an interaction between the divacancy orbitals and the Si-impurity states. The Si impurity has six immediate-neighbor C atoms in divacancy. The calculated distance between Si and C atoms is about 1.97 Å in the neutral charge state, which is longer than the usual Si-C covalent bond (1.88 Å). Since C atoms are more electronegative than Si atoms the charge transfer from the Si atom toward the C atoms can be relatively large, leaving positively charged Si ion behind. The divacancy has D_{3d} symmetry with six C dangling bonds. These dangling bonds form a_{1g}, a_{2u}, e_u, and e_g orbitals, while the Si-related four sp^3 states should form a_{1g}, e_u, and

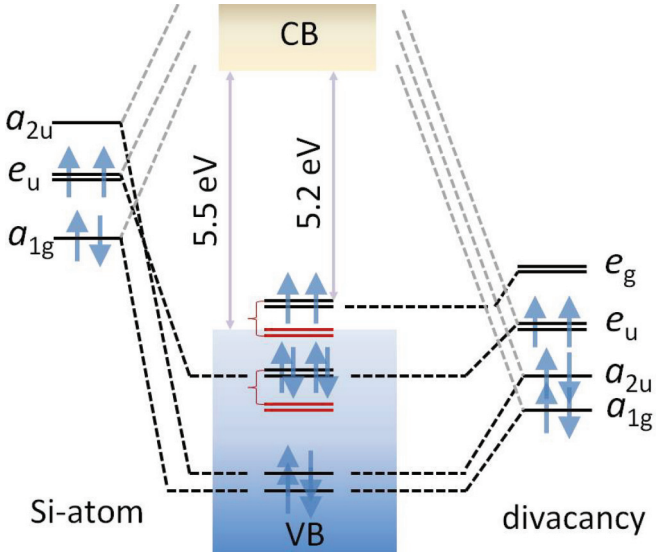

FIG. 2. (Color online) The defect-molecule diagram of the neutral SiV defect in diamond. The irreducible representation of the orbitals under D_{3d} symmetry is shown. The orbitals of the Si-atom and the six carbon dangling bonds of divacancy recombine in diamond where the conduction band (CB) and valence band (VB) are schematically depicted. The e_g orbital is very close to the VB maximum, forming a strong resonance state at the VB edge shown as brown (lighter gray) lines. The e_u level falls in the VB that also forms a strong resonance even deeper in the VB. For the sake of simplicity, the position of the spin-up (majority spin channel) levels are depicted in the spin-polarized DFT calculation.

a_{2u} orbitals in D_{3d} crystal field (the explicit form of these orbitals as a function of sp^3 states can be seen in Ref. 35). Please note that the a_{1g}, a_{2u} and e_u states may be combined, but e_g orbitals should be pure C dangling bond states (see Fig. 2). The bonding and antibonding combinations of these states form the defect states of SiV defect. According to HSE06 calculation the occupation of the defect states may be described as $a^2_{1g}a^2_{2u}e^4_u e^2_g$, which agrees again with previous LDA calculations.[4,34] Here, the ten electrons are coming from the six electrons of C dangling bonds and the four sp^3 electrons of the Si impurity. As two electrons occupy the double degenerate e_g state, the high-spin $S = 1$ ground state naturally forms by following Hund's rules. It is important to determine the position of the defect levels. Interestingly, HSE06 predicts that only e_g appears in the band gap. In the spin-polarized calculation the occupied e_g state in the spin-up channel is at $E_{\rm VBM} + 0.3$ eV. The e_u state is resonant with the VB and can be found just 0.64 eV below VBM. The occupied a_{1g} state lies very deep in the VB and may play no important role in the excitation or ionization processes. Our estimations indicate that the a_{2u} defect level is too deep in the VB to be excited by red excitation. However, higher energetic lasers (in the green and blue spectrum) can excite this state and other states within the VB with a_{2u} symmetry. The empty antibonding orbitals fall in the CB, and will not be considered any more. The most important e_u and e_g states are depicted in Fig. 3. Although the e_u state lies in the VB, it is still localized around the defect site. The VB states are strongly perturbed by the presence of the defect. The VBM is triple degenerate in a perfect lattice that

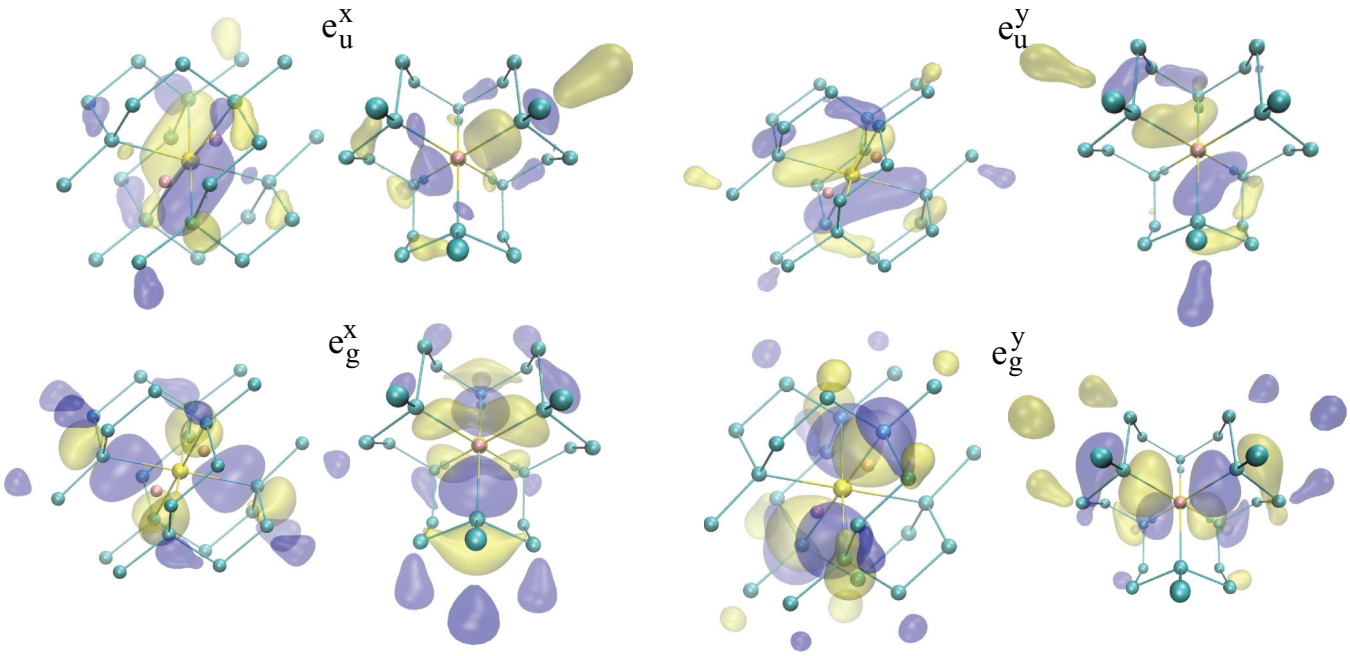

FIG. 3. (Color online) The electron wave function of e_u and e_g defect states in the neutral SiV defect. Both states are double degenerate, so both x and y components are depicted. Note that e_u states are changing sign upon inversion while e_g states do not, as their irreducible representation indicates. Furthermore, Si orbitals have little contribution in the e_u state but no contribution to the e_g state. The e_u state is resonant with the VB, thus less localized, whereas the localized e_g state lies in the band gap.

splits to an upper a_{1g} level and a lower e_g level in the presence of the defect. Since this $e_{g(\mathrm{VBM})}$ state has the same symmetry as the low-lying e_g defect state, that $e_{g(\mathrm{VBM})}$ state becomes a defect resonance state. Similar phenomena occur for the deep e_u defect state as well. The shallow $e_{g(\mathrm{VBM})}$ state may play an important role in the excitation/deexcitation process of the defect.

We conclude that the neutral SiV defect (i) has $^3A_{2g}$ ground state, (ii) can be theoretically ionized as (2+) and (1+), as well as (1−) and (2−), by emptying or filling the double degenerate e_g state in the gap. While the concept of Fermi level could have limitations in wide-band-gap diamond[36] boron and nitrogen impurities may provide holes and electrons to the diamond crystal, respectively, so that the SiV defect might be positively or negatively charged. In order to establish the relevant charge states, one has to calculate the adiabatic charge transition levels of SiV defect.

B. Charge transition levels of SiV defect in diamond

We found that the neutral, negatively charged, and double negatively charged states can be found in diamond (see Fig. 4). The single positively charged state might be only found in very highly p-type doped diamond samples. The calculated $(-|0)$ level at $E_{\mathrm{VBM}} + 1.43$ eV is very close to the level that is associated with the acceptor ionization energy of the defect from photoconductivity measurements at $\sim E_{\mathrm{VBM}} + 1.5$ eV (Ref. 15). Interestingly, the calculated $(2-|-)$ level at $\sim E_{\mathrm{VBM}} + 2.14$ eV is well below the midgap. Since the e_g level is fully occupied at $E_{\mathrm{VBM}} + 1.5$ eV in (2−) charge state, intralevel optical transition cannot take place, and ultraviolet excitation (∼4.0 eV) is needed to excite or ionize the defect optically to the CB edge. Another important note that the calculated acceptor level of NV lies at $\sim E_{\mathrm{VBM}} + 2.6$ eV (Refs. 20 and 37). This means that if both NV and SiV defects are present in the diamond sample, then most of the NV defects should be neutral in order to detect SiV^- defect. Another important point is that the luminescence from SiV^- defect can be more stable than that of NV^- defect in nanodiamonds as a function of surface termination because the corresponding $(2-|-)$ charge transition level lies deeper in the band gap

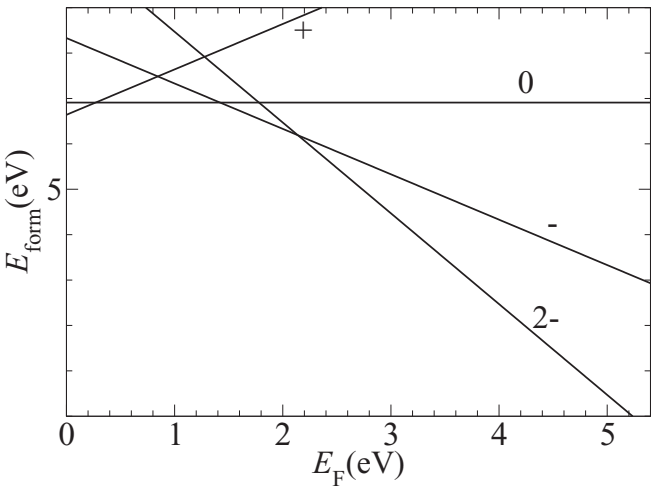

FIG. 4. The calculated formation energy of SiV defect as a function of the Fermi level in the gap. The crossing points represent the charge transition levels. The chemical potential of Si is taken from cubic silicon carbide in the carbon-rich limit.

than the $(-|0)$ level of NV defect. All in all, the neutral and negatively charged SiV defects are relevant for intralevel optical transitions.

C. Negatively charged SiV defect in diamond: Analysis of the ground and excited states and the zero-phonon-line energy

In the negatively charged SiV defect the ground-state electron configuration is $e_u^4 e_g^3$. This is principally a Jahn-Teller unstable system as the double degenerate e_g level is partially filled (in the spin-down channel in our calculation). This has ^2E_g symmetry in D_{3d} symmetry. In HSE06 geometry optimization we allowed the systems to relax to lower symmetries. Indeed, HSE06 showed a C_{2h} distortion where two C atoms have 0.03-Å longer distance from Si atom than the other two atoms. In this particular case ^2B_g state was formed in C_{2h} symmetry. However, we have to note that the dynamic coupling between vibrations and electronic states cannot be taken into account in our calculation. Thus, the dynamic Jahn-Teller system cannot be directly described by our method. For instance, static Jahn-Teller effect occurs for NV^0 in Ref. 38 while it is known from experiments that it is a dynamic Jahn-Teller system. Since the distortion from D_{3d} symmetry obtained by HSE06 calculation is small, the defect may well have D_{3d} symmetry with the dynamic Jahn-Teller effect. We note that no such EPR center with $S = 1/2$ spin was found that could be associated with SiV defect. This also hints that the ground state of SiV^- is a dynamic Jahn-Teller system which prohibits the electron spin resonance signal similar to NV^0 defect.

Now, we discuss the possible excited states of this system. Again, the fully occupied e_u state is resonant with the VB. Still, one electron from this level may be promoted to the e_g level in the band gap. The resulting ^2E_u excited state is again Jahn-Teller unstable. Interestingly, when the electron from the minority spin-down e_u level in the VB was promoted to the e_g state in the gap, then the resulting hole state pops up clearly above the VB edge at about $E_{\mathrm{VBM}} + 0.12$ eV [see Fig. 5(a)]. This hole state is definitely localized and may result in sharp transition in the luminescence process. The $^2E_u \rightarrow {}^2E_g$ optical transition is allowed. In HSE06 calculation the excited state has also C_{2h} distortion but the effect is again small and can be a dynamic Jahn-Teller system. The calculated ZPL energy is about 1.72 eV, which agrees well with that of 1.68-eV PL center. The calculated relaxation energy due to optical excitation is about 0.03 eV, which is much smaller than that of the NV center (about 0.21 eV), and explains the small contribution of the vibration sideband in the emission spectrum. Thus, the assignment of the 1.68-eV PL center with SiV^- defect is well supported by our calculation: The calculated ZPL energy, the small Stokes shift, and the possibility of dynamic Jahn-Teller effect agree with the known properties of the 1.68-eV PL center.

We further argue that the sharp ZPL of SiV^- as well as the relative strength of the fine-structure splittings in the ground and excited states can be well understood by our findings. The ^2E_g ground and ^2E_u excited states have very similar electron charge densities, where mostly just the phase differs between the two states. As a result, the ions will be subject to similar

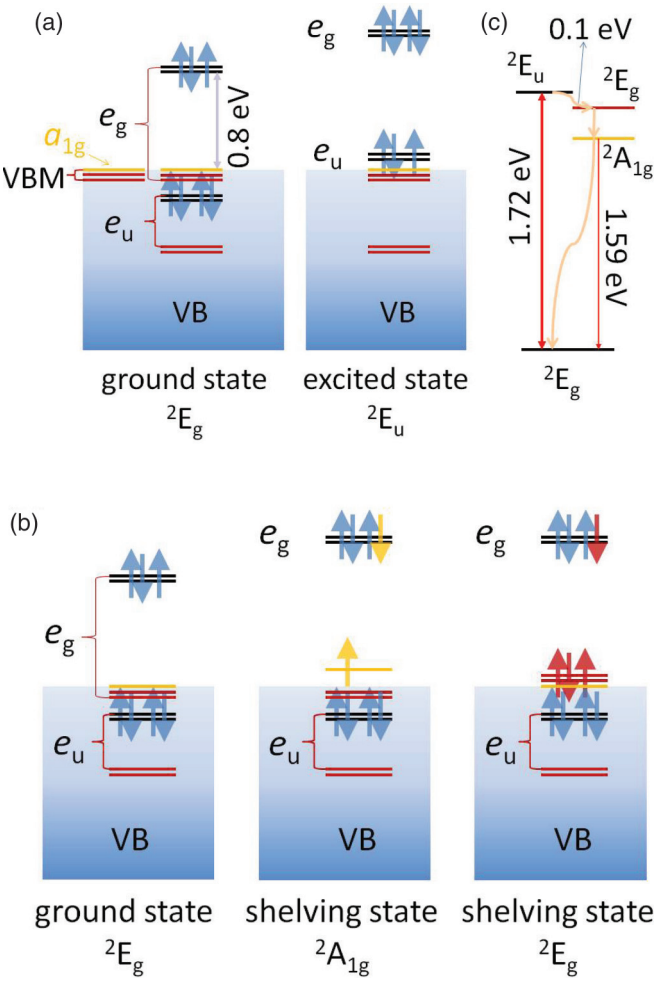

FIG. 5. (Color online) Schematic diagram about the electronic structure of the negatively charged SiV defect in diamond. The valence band (VB) resonant states play a crucial role in the excitation. For the sake of the simplicity, the spin polarization of the single-particle levels are not shown. (a) Ground and the bright (optically allowed) excited state. (b) Ground and shelving states when the hole is left on the split VB edge states. (c) Schematic energy level diagram based on HSE06 constraint DFT calculations. Thick red lines indicate strong absorption/emission while the thin red line indicates a weak radiative recombination in the case of the presence of strain which breaks the inversion symmetry of the defect. Orange wavy arrows represent nonradiative recombination down to the ground state.

potentials in their ground and excited states, leading to only a small change in the geometry due to optical excitation. This is in stark contrast to the case of NV^- defect where the electron charge density strongly redistributes upon optical excitation, leading to a large Stokes shift.[18] Another observation is that the ^2E_g state virtually is not localized at all on the Si atom due to symmetry reasons; however, our projected density-of-states analysis shows that there is a small contribution from the orbitals of the Si atom in the ^2E_u excited state, allowed by symmetry. This may explain the larger splitting in the fine structure of the excited state than that in the ground state:[3] The ^2E_u state has expected to have larger spin-orbit splitting due to the small contribution of the orbitals of the Si atom than that in

^2E_g state, where this contribution is missing, as the spin-orbit strength increases with the atomic number to the fourth power.

Furthermore, our HSE06 calculations reveal that the heavily perturbed VB edges can play important role in understanding the defect properties as those states lie closer to the e_g state in the band gap than the e_u resonant defect state. Therefore, we calculate the excitation from the split VBM states. A ^2E_g excited state and a $^2A_{1g}$ excited state are built from the hole left on the $e_{g(\mathrm{VBM})}$ and $a_{1g(\mathrm{VBM})}$ states, respectively [cf., Fig. 5(b)]. We find that the ^2E_g excited state is ∼0.1 eV lower in energy than the bright ^2E_u excited state where the calculated Stokes shift of this transition is again small. The $^2A_{1g}$ excited state is ∼1.59 eV above the ^2E_g ground state. In the latter case the hole level is again at $\sim E_{\mathrm{VBM}} + 0.11$ eV, which may result in sharp transition in the luminescence if it becomes an allowed process.

These results can explain the nature of the shelving state in 1.68-eV PL center. Unlike the NV center the SiV defect has inversion symmetry that plays a crucial role in the deexcitation process. Due to the inversion symmetry, the ^2E_g and $^2A_{1g}$ excited states are shelving states because they are optically forbidden due to the same parity of their wave function with that of the ground state. Thus, the shelving states have the same spin state as the ground and the bright excited states. Since the ^2E_g shelving state has a level very close to that of the bright ^2E_u state, the nonradiative coupling between these states can be efficient. We further note that a new and weak near-infrared (NIR) transition at ∼823 nm (1.52 eV) has been found associated with the negatively charged SiV defect.[39] The measurements implied that this transition belongs to the same charge as the 1.68-eV transition. This NIR transition was particularly found in ensemble measurements of nanodiamond samples when strain was present in the sample.[39] Our calculations imply [Fig. 5(c)] that this weak radiative transition can be explained by the slightly distorted $^2A_{1g}$ excited state. Any distortion of the diamond lattice will break the inversion symmetry of the SiV defect, so the parity of the corresponding wave functions. Therefore, transitions between $^2A_1$ and ^2E (originally $^2A_{1g}$ and ^2E_g) will be allowed. The calculated transition energy (1.59 eV) is very close to the detected one, which further supports our assignment. Our calculations highlight the importance of the VB edge states in understanding the optical properties of a 1.68-eV center in diamond.

We note again that the e_u state is resonant with the VB. Thus, unlike the case of the NV center with well-separated atomiclike states in the gap, it is probable that ionization of the defect can occur during optical excitation. In this process, a hole is created that might (temporarily) leave the defect with creating an optically inactive (2−) charge state, particularly in the presence of external perturbations that create an effective electric field. This (2−) charge state can be optically converted back to (−) state only by ultraviolet excitation.

D. Neutral SiV defect: Hyperfine tensors and zero-phonon-line energy

The (2−) charge state is a closed-shell singlet while the neutral and negatively charged SiV defects have $S = 1$ and $S = 1/2$ spin states, respectively. The SiV^0 defect was assigned to KUL1 EPR center with $S = 1$ state and D_{3d} symmetry.[13,34] Our calculations support this assignment (see Table I). The spin density is localized on four C dangling bonds in the e_g orbital of divacancy. While the e_g state is not localized on Si impurity but the spin density from these C dangling bonds can overlap with the Si atom, which promotes a well measurable Fermi-contact term on the ^{29}Si nuclei. The hyperfine interaction with ^{29}Si is almost isotropic, unlike the case of ^{13}C isotopes which show typical anisotropic signal due to sp^3 dangling bonds. The calculated and measured ^{13}C hyperfine tensor agree very well. We note that the contribution of the spin-polarization of core electrons to the Fermi-contact term is very significant, which *compensates* the hyperfine interaction due to valence electrons. We found this effect also for NV and other related defects.[30]

Next, we discuss the optical transitions for SiV^0. Intralevel transition may occur between the fully occupied e_u state and the empty e_g state in the spin-down channel. While the fully occupied e_u state lies in the VB a strong resonant excitation may occur from this state. In the hole picture the excited state may be described as $e_u^1 e_g^1$ while the ground state is e_g^2. The electron configuration of e_g^2 results in the $^3A_{2g}$ triplet state and the ^1E_g and $^1A_{1g}$ singlet states. The ground state is $^3A_{2g}$. The electron configurations of $e_u^1 e_g^1$ results in $^3A_{1u}$, $^1A_{1u}$, $^3A_{2u}$, $^1A_{2u}$, ^3E_u, and ^1E_u multiplets. Among these states the $^3A_{1u}$ and ^3E_u states are optically allowed from the $^3A_{2g}$ ground state. Polarization studies of the 1.31-eV center indicates that $^3A_{1u} \rightarrow {}^3A_{2g}$ transition occurs in the PL process.[14] The $^3A_{1u}$ state can be described as a linear combination of Slater determinants that cannot be treated within constraint DFT. However, the $M_S = 1$ substate of a ^3E_u multiplet can be described by a single Slater determinant. The calculated excitation energy is about 1.63 eV, which is significantly larger than 1.31 eV. Thus, we may conclude that the $^3E_u \rightarrow {}^3A_{2g}$ transition is not responsible for the 1.31-eV PL line. As the only other feasible transition is $^3A_{1u} \rightarrow {}^3A_{2g}$, our result indirectly confirms the experimental finding.

We also study the role of the VB resonant states similar to the case of the negatively charged defect. When the electron is promoted from the $a_{1g(\mathrm{VBM})}$ state to the e_g state in the gap, then the ^3E_g state is created. The calculated excitation energy of this shelving state is ∼1.27 eV. This coincides with the small peak found in Ref. 14, simultaneously with the peak of 1.31 eV. This transition is optically allowed only when the inversion symmetry of the defect is broken. This might happen due to strain in the diamond sample. Nevertheless, our calculation implies that this ^3E_g state can play an important role in the deexcitation process as a shelving or metastable state.

We note that the experiments indicate[14] that the ground state of the neutral SiV defect resides at ∼0.2 eV above the VB edge. According to HSE06 calculations the occupied single-particle e_g level lies at $E_{\mathrm{VBM}} + 0.3$ eV, which agrees nicely with the implications from the experiments. In addition, we found a metastable state of the defect which may explain the temperature dependence of the 1.31-eV PL spectrum.[14] We also propose that strain may induce a weak PL transition from this shelving state because this shelving state has the same spin as that of the ground state, and the parity selection rule may be relaxed in slightly distorted geometry of the SiV defect. We

further note that a very similar conclusion can be drawn for the optical excitation of the neutral SiV defect, as was hinted for the negatively charged defect: A hole is created in the VB in the excitation process that may leave defect temporarily or permanently, which leads to a charge conversion from neutral to negatively charged SiV defect.

IV. SUMMARY AND CONCLUSION

We carried out *ab initio* supercell calculations on SiV defect in diamond. The calculations could positively confirm the assignment of 1.68- and 1.31-eV PL centers to the negatively charged and neutral SiV defects, respectively. The calculations reveal the high importance of the inversion symmetry of the center as well as the role of resonant VB states in understanding the optical properties of the defect. We show that the shelving states of the 1.68-eV PL center are from VB excitations where the lowest-energy shelving state may have NIR emission to the ground state in strain diamond samples. We show that holes are created in the excitation of the negatively charged and neutral SiV defects that may lead to charge conversion of these centers. In addition, we show that the acceptor level of the SiV defect lies very deep in the band gap. As a consequence, the 1.68-eV PL center can be photostable when it is close to the surface of the hydrogenated diamond surface. On the other hand, the SiV defect is double negatively charged in such diamond samples where the NV defect is negatively charged. Thus, the Fermi level should be set lower than the midgap of diamond, in order to conserve its negatively charged state.

ACKNOWLEDGMENTS

Discussions with Christoph Becher, Fedor Jelezko, and Jonathan Goss are highly appreciated. Support from EU FP7 Project DIAMANT (Grant No. 270197) is acknowledged. J.R.M. acknowledges support from Conicyt PIA Program No. ACT1108.

*agali@eik.bme.hu
†jeromaze@gmail.com

[1] V. S. Vavilov, A. A. Gippius, B. V. Zaitsev, B. V. Deryagin, B. V. Spitsyn, and A. E. Aleksenko, Fiz. Tekh. Polopruvodn. **14**, 1811 (1980) [Sov. Phys. Semicond. **14**, 1078 (1980)].
[2] A. M. Zaitsev, V. S. Vavilov, and A. A. Gippius, Sov. Phys. Lab. Inst. Rep. **10**, 15 (1981).
[3] C. D. Clark, H. Kanda, I. Kiflawi, and G. Sittas, Phys. Rev. B **51**, 16681 (1995).
[4] J. P. Goss, R. Jones, S. J. Breuer, P. R. Briddon, and S. Öberg, Phys. Rev. Lett. **77**, 3041 (1996).
[5] C. Wang, C. Kurtsiefer, H. Weinfurter, and B. Burchard, J. Phys. B **39**, 37 (2006).
[6] E. Neu, D. Steinmetz, J. Riedrich-Möller, S. Gsell, M. Fischer, M. Schreck, and C. Becher, New J. Phys. **13**, 025012 (2011).
[7] E. Neu, M. Fischer, S. Gsell, M. Schreck, and C. Becher, Phys. Rev. B **84**, 205211 (2011).
[8] E. Neu, C. Hepp, M. Hauschild, S. Gsell, M. Fischer, H. Sternschulte, D. Steinmüller-Nethl, M. Schreck, and C. Becher, New J. Phys. **15**, 043005 (2013).
[9] A. S. Barnard, I. I. Vlasov, and V. G. Ralchenko, J. Mater. Chem. **19**, 360 (2009).
[10] S. Moliver, Tech. Phys. **48**, 1449 (2003).
[11] K. Iakoubovskii, A. Stesmans, B. Nouwen, and G. J. Adriaenssens, Phys. Rev. B **62**, 16587 (2000).
[12] K. Iakoubovskii and A. Stesmans, Phys. Rev. B **66**, 195207 (2002).
[13] A. M. Edmonds, M. E. Newton, P. M. Martineau, D. J. Twitchen, and S. D. Williams, Phys. Rev. B **77**, 245205 (2008).
[14] U. F. S. D'Haenens-Johansson, A. M. Edmonds, B. L. Green, M. E. Newton, G. Davies, P. M. Martineau, R. U. A. Khan, and D. J. Twitchen, Phys. Rev. B **84**, 245208 (2011).
[15] L. Allers and A. T. Collins, J. Appl. Phys. **77**, 3879 (1995).
[16] J. P. Perdew and A. Zunger, Phys. Rev. B **23**, 5048 (1981).
[17] A. Gali, Phys. Status Solidi B **248**, 1337 (2011).
[18] A. Gali, E. Janzén, P. Deák, G. Kresse, and E. Kaxiras, Phys. Rev. Lett. **103**, 186404 (2009).
[19] P. Deák, B. Aradi, T. Frauenheim, E. Janzén, and A. Gali, Phys. Rev. B **81**, 153203 (2010).
[20] P. Deák, B. Aradi, M. Kaviani, T. Frauenheim, and A. Gali, arXiv:1311.6598 [Phys. Rev. B (to be published)].
[21] F. Fuchs, J. Furthmüller, F. Bechstedt, M. Shishkin, and G. Kresse, Phys. Rev. B **76**, 115109 (2007).
[22] J. Heyd, G. E. Scuseria, and M. Ernzerhof, J. Chem. Phys. **118**, 8207 (2003).
[23] A. V. Krukau, O. A. Vydrov, A. F. Izmaylov, and G. E. Scuseria, J. Chem. Phys. **125**, 224106 (2006).
[24] P. E. Blöchl, Phys. Rev. B **50**, 17953 (1994).
[25] G. Kresse and J. Furthmüller, Phys. Rev. B **54**, 11169 (1996).
[26] J. P. Perdew, K. Burke, and M. Ernzerhof, Phys. Rev. Lett. **77**, 3865 (1996).
[27] H. J. Monkhorst and J. K. Pack, Phys. Rev. B **13**, 5188 (1976).
[28] P. Deák, A. Gali, B. Aradi, and T. Frauenheim, Phys. Status Solidi B **248**, 790 (2011).
[29] P. E. Blöchl, Phys. Rev. B **62**, 6158 (2000).
[30] K. Szász, T. Hornos, M. Marsman, and A. Gali, Phys. Rev. B **88**, 075202 (2013).
[31] O. V. Yazyev, I. Tavernelli, L. Helm, and U. Röthlisberger, Phys. Rev. B **71**, 115110 (2005).
[32] S. Lany and A. Zunger, Phys. Rev. B **78**, 235104 (2008).
[33] H.-P. Komsa, T. T. Rantala, and A. Pasquarello, Phys. Rev. B **86**, 045112 (2012).
[34] J. P. Goss, P. R. Briddon, and M. J. Shaw, Phys. Rev. B **76**, 075204 (2007).
[35] C. Hepp, T. Müller, V. Waselowski, J. N. Becker, B. Pingault, H. Sternschulte, D. Steinmüller-Nethl, A. Gali, J. R. Maze, M. Atatüre, and C. Becher, arXiv:1310.3106 [Phys. Rev. Lett. (to be published)].
[36] A. T. Collins, J. Phys.: Condens. Matter **14**, 3743 (2002).
[37] N. Mizuochi, T. Makino, H. Kato, D. Takeuchi, M. Ogura, H. Okushi, M. Nothaft, P. Neumann, A. Gali, F. Jelezko, J. Wrachtrup, and S. Yamasaki, Nat. Photon. **6**, 299 (2012).
[38] A. Gali, Phys. Rev. B **79**, 235210 (2009).
[39] E. Neu, R. Albrecht, M. Fischer, S. Gsell, M. Schreck, and C. Becher, Phys. Rev. B **85**, 245207 (2012).